REVIEW

Check for updates

Advances in hydroformylation with formaldehyde, formic acid and carbon dioxide as syngas surrogates

Zerun Zhao, [ID] *[ab] Shuai Lei,[ac] Wanru Feng,[a] Xingyong Wang,[a] Hongchen Li,[a] He Chen,[a] Lu Wang,[a] Fujun Zhao[a] and Songbao Fu*[a]

Hydroformylation, a catalytic transformation of alkenes into aldehydes using CO/H_2, represents a fundamental route for the valorization of olefins in both industrial and academic settings. To address the safety and sustainability concerns associated with the direct use of carbon monoxide, recent research has increasingly focused on the development of C_1-based carbonyl surrogates. In particular, formaldehyde, formic acid, and carbon dioxide have been investigated as viable alternatives capable of releasing CO *in situ* under appropriate catalytic conditions. These strategies have led to the emergence of "syngas-free" hydroformylation processes, which offer new possibilities for reaction design and system integration. This review provides a comprehensive overview of recent developments in the use of formaldehyde, formic acid, and CO_2 as carbonyl surrogates in transition metal-catalyzed hydroformylation, highlighting advances in homogeneous and heterogeneous catalytic systems, substrate scope, and reaction mechanism.

Introduction

Transition-metal-catalyzed hydroformylation of olefins was first reported by Roelen in 1938 and has since remained one of the most important carbonylation processes in both industrial and academic contexts.[1,2] Currently, more than ten million tons of aldehydes are produced annually from alkenes *via* hydroformylation.[3] These aldehydes serve as key intermediates in the synthesis of various value-added chemicals—such as alcohols, carboxylic acids, esters, and acetals—that are extensively applied in the production of surfactants, lubricant additives, and polymeric materials.[1] Traditionally, syngas has been the predominant C1 feedstock for hydroformylation, and classic hydroformylation typically requires elevated pressures of syngas and delivers mixtures of linear and branched aldehydes. Accordingly, considerable research has focused on catalyst/ligand design to maximize linear selectivity and activity. Despite its remarkable success, conventional hydroformylation remains heavily dependent on externally supplied CO/H_2, a reliance that poses notable challenges in both safety and sustainability. Carbon monoxide, being colorless, flammable, and highly toxic, demands stringent handling protocols and

specialized high-pressure equipment to ensure operational safety. In addition, syngas is conventionally produced from fossil feedstocks, further intensifying environmental concerns and stimulating the search for alternative, renewable carbon sources within the framework of green chemistry.

In response to these challenges, over the past two decades significant efforts have been devoted to developing alternative "CO-free" strategies. Morimoto's review in 2004 highlighted the initial forays into carbonylation with CO surrogates, setting the stage for a series of breakthroughs.[4] Some ideal CO surrogates should be easy to transport and readily derived from waste biomass, such as HCHO, HCOOH, CH_3OH and so on. Beller and Skrydstrup's groups reported a coupled catalytic system that integrates Ru-catalyzed methanol-to-syngas reforming with Rh-catalyzed hydroformylation of olefins, underscoring its potential in the transition from fossil-based to renewable resources.[5] Methanol-related studies, however, were not addressed in detail in this review. The common strategy is to pair such a surrogate with a multifunctional catalyst system capable of decomposing or transforming the surrogate into CO (and H_2 or a hydride species) and subsequently carrying out the hydroformylation reaction. In recent years, multiple reviews and monographs have addressed various aspects of the general hydroformylation process, but detailed discussions of syngas surrogates were scarce. Herein, we provide a comprehensive overview of the latest advancements in hydroformylation protocols employing formaldehyde, formic acid and CO_2/H_2 as CO surrogates, with particular emphasis on their applications in complex organic synthesis and pharmaceutical development.

[a] CNOOC Institute of Chemicals & Advanced Materials, CNOOC, Beijing 102209, China. E-mail: zhaozr5@cnooc.com.cn; fushb@cnooc.com.cn

[b] School of Chemistry and Chemical Engineering, Nanjing University, 163 Xianlin Avenue, Nanjing, 210023, Jiangsu, P. R. China

[c] State Key Laboratory of Heavy Oil Processing, China University of Petroleum (East China), Qingdao, China

Formaldehyde as carbonyl source

Rhodium-catalyzed hydroformylation of olefins with formaldehyde has emerged as an innovative route to access a diverse array of substituted aldehydes.[6-8] In these systems, formaldehyde was typically introduced as formalin solution or paraformaldehyde. This method usually comprises two synergistic catalytic steps: first, the decarbonylation of formaldehyde to generate an active carbonyl species and hydrogen, which used in the subsequent hydroformylation of alkenes, and the corresponding reactions were performed in a batch reactor via a one-pot procedure.

The first example using formaldehyde was demonstrated by Okano and co-workers in 1982 that $[RhH_2(O_2COH)(PiPr_3)_2]$ (iPr: isopropane) catalyzed the hydroformylation of 1-hexene, affording the aldehyde in 67% yield alongside minor alcohol.[6] Over the past decades, this field has witnessed sustained progress and methodological advances. In 2009, Morimoto reported a highly linear-selective hydroformylation of 1-alkenes using formal-dehyde as a syngas substitute[9] (Fig. 1). In this case, a catalyst system derived from commercially available [Rh(COD)Cl]$_2$ in combination with BIPHEP (2,2′-bis(diphenylphosphino)-1,1′-biphenyl) and Nixantphos (4,6-bis(diphenylphosphino) phenoxazine) had stand out. For 1-decene, the reaction had a 95% GC yield with excellent regioselectivity (linear/branched = 97 : 3) at 90 °C for 20 h. And 1-octene also proceeded well to give nonanal (linear) and 2-methyloctanal (branched) with 90% yield in a ratio of l/b = 97/3. Subsequently, building on the Rh(ɪ)/BINAP/Xantphos (BINAP: rac-2,2′-bis(diphenylphosphino)-1,1′-binaphthyl, Xantphos: 9,9-dimethyl-4,5-bis(diphenylphosphino)xanthene) catalytic system, Taddei and co-workers developed a microwave-assisted hydroformylation protocol[10] (Fig. 1). For both simple and functionalized alkenes, microwave heating shortened reaction time from over 10 hours to just 30 minutes while preserving high yields and selectivity. Encouraged by these results, they applied the optimized system to substrates prone to double-bond isomerization and carbonyl conjugation, for example α- and γ-unsaturated amides, and obtained the desired cyclized products in 89% yield using [Rh(COD)Cl]$_2$/BIPHEP/Xantphos under microwave conditions.

Bearing the known dependency of some Rh-catalyzed hydroformylations with syngas on the hydrogen partial pressure in mind, In 2013, Börner and coworkers described Rh-dppp(1,3-bis(diphenylphosphino)propane)-catalyzed hydroformylation with formaldehyde and an external H$_2$-source.[11] They observed that addition of 10 bar of hydrogen could significantly improve the regioselectivity and accelerate the reaction. In particular, for styrene and its derivatives, the presence of hydrogen increased aldehyde yields by over fivefold. In this case, the additional hydrogen promoted the hydrogenolysis of the Rh–acyl complex in the catalytic cycle.

Asymmetric hydroformylation offers an exceptionally efficient route to bioactive compounds and pharmaceutically active compounds, furnishing enantioselective aldehydes that serve as valuable precursors for fine chemicals and drug synthesis.[12,13] In 2015, Morimoto and co-workers attempted the asymmetric hydroformylation of alkenes using formaldehyde as the carbonyl source[14] (Fig. 2). Initially, the reactivity of vinylarenes was probed by screening a range of chiral phosphine ligands—(S)-BINAP, (S,S)-BDPP ((2S,4S)-(−)-2,4-bis(diphenylphosphin) pentane), (S,S)-BPE ((+)-1,2-bis((2S,5S)-2,5-diphenylphospholano)ethane), (R,R)-BPE (1,2-bis((2R,5R)-2,5-diphenylphospholano)ethane), and others. Outstanding

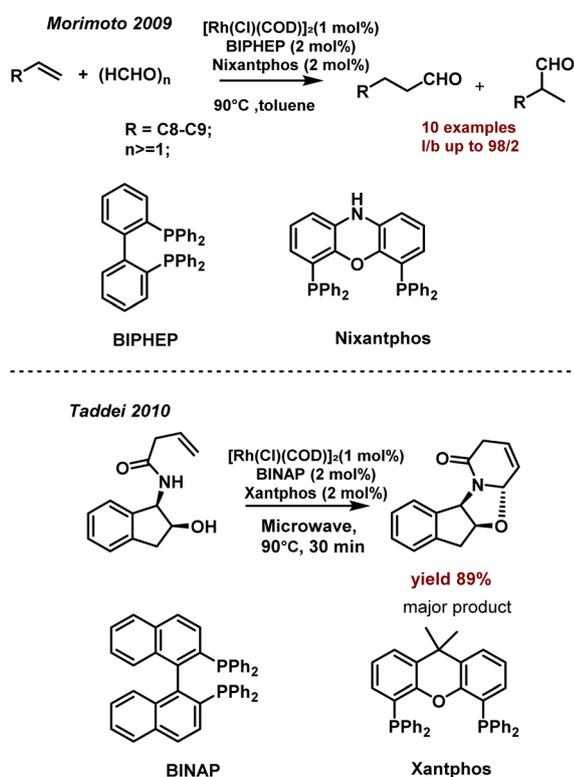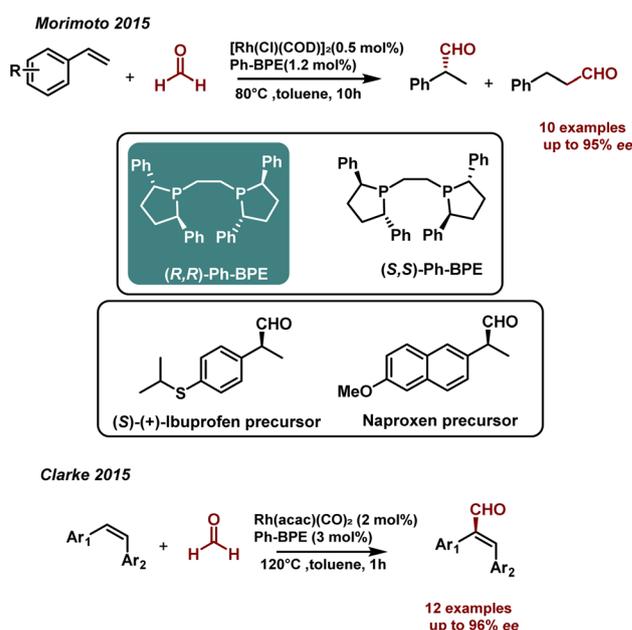Fig. 1 [Rh(COD)Cl]$_2$-catalyzed hydroformylation of olefins and functionalized alkenes with HCHO.

Fig. 2 Rh–Ph–BPE-catalyzed asymmetric hydroformylation.

regioselectivities (*b*/*l* up to 96 : 4) and enantioselectivities (up to 95% ee) were achieved using the [Rh(COD)Cl]$_2$/Ph–BPE catalytic system. They further applied this protocol to the synthesis of pharmaceutical precursors, achieving high yields with excellent regio- and enantioselectivities. Based on these findings, Clarke's group developed a rapid asymmetric hydroformylation (ATHF) method of disubstituted alkenes[15] (Fig. 2). They employed a catalytic system composed of Rh(acac)(CO)$_2$ and Ph–BPE, which delivered excellent activity and enantioselectivity (up to 96% ee). While the aforementioned catalytic system delivered high enantioselectivity in the ATHF, it still faced the challenge of suboptimal yields or regioselectivity, particularly with *cis*-stilbene derivatives as substrates. In 2019, Clarke's group carried out a more in-depth study of the Rh/Ph–BPE-catalyzed asymmetric hydroformylation and developed a dual-catalyst system to address this problem.[16] In this method, formaldehyde was first decomposed into CO and H$_2$ by a [Rh(COD)Cl]$_2$/Ph–BPE, after which Rh(acac)(CO)$_2$ was introduced to form a conventional hydroformylation system with pre-added Ph–BPE. Under optimized conditions, a series of previously challenging substrates exhibited markedly improved regioselectivity, enantiomeric excess (e.e.), and diastereomeric ratio (d.r.) compared to the original ATHF protocol. Under typical asymmetric hydroformylation conditions, this protocol delivered superior conversions, enantioselectivities and regioselectivity for certain less-activated substrates, outperforming both the same and other catalysts employed in conventional methods. This advantage renders it a valuable tool for synthetic chemists in constructing chiral aldehydes.

Morimoto's reaction conditions have been applied in substrates including linear alkenes, functionalized alkenes, aromatic alkenes, and some pharmaceutical precursors, but β-functionalized olefins have not been investigated, *e.g.* cyanide. In hydroformylation reactions, calculating the natural P–M–P bite angles of bidentate diphosphine ligands are crucial for understanding their influence on regioselectivity. It can be exerted by two different effects described as the steric bite angle effect and the electronic bite angle effect. In 2018, Lühr and co-workers explored how the natural bite angle of bidentate diphosphine ligands influenced the branched hydroformylation of β-functionalized olefins, employing formaldehyde as a syngas surrogate[17] (Fig. 3). They screened a series of Xantphos-type and

alkyl diphosphine ligands with bite angles (β_n) spanning 86° to 114°, and using olefins bearing cyanide groups as substrates. They revealed that the reaction's regioselectivity was predominantly dictated by the natural bite angles (β_n) of these bidentate ligands, which the smaller bite angles ($\beta_n = 86°$ and 91°) preferentially yield branched aldehydes, whereas those with larger angles ($\beta_n = 108°$ and 114°) favor the formation of linear aldehydes.

In the past years, the valorization of renewable biomass into high-value chemicals has become a prominent research frontier.[18] Allylbenzene derivatives, prized in the flavor, food, and pharmaceutical sectors, as well as building blocks for the construction of complex molecules.[19] In 2022, the Lühr group reported a follow-up study focused on the transfer hydroformylation and isomerization of biobased olefins using formaldehyde as a CO/H$_2$ surrogate[20] (Fig. 4). It has been demonstrated that catalytic performance critically depended on the synergy between the metal precursor and the ligand: the [Rh(COD)Cl]$_2$/*rac*-BINAP/PPh$_3$ (triphenylphosphine) system efficiently promotes aldehyde formation, whereas [Rh(acac)(CO)$_2$]/PPh$_3$ favors isomerization with excellent *E*/*Z* control (*E*/*Z* > 99 : 0). Mechanistic investigations further revealed the generation of active rhodium–hydride species, and elucidated the possible hydrogen-transfer and β-elimination pathways operative in the catalytic cycle. Moreover, by tuning the natural bite angle (β_n) of bidentate diphosphine ligands, they achieved markedly enhanced regioselectivity for linear aldehydes (*l*/*b* up to 94 : 6). This work not only broadened the scope of syngas-free hydroformylation but also provides a green and efficient route to valuable arylpropanal derivatives, with significant theoretical and practical implications.
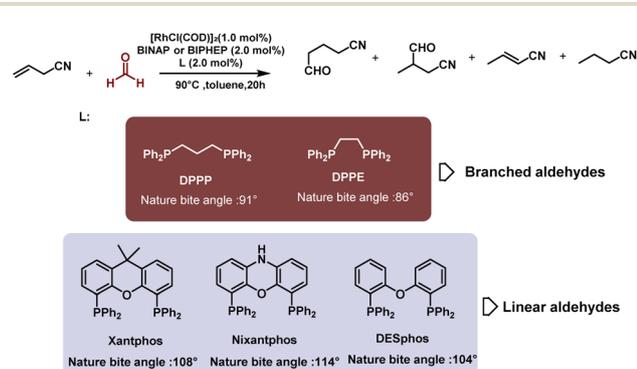

Fig. 3 Rh-catalyzed hydroformylation of β-functionalized olefins.
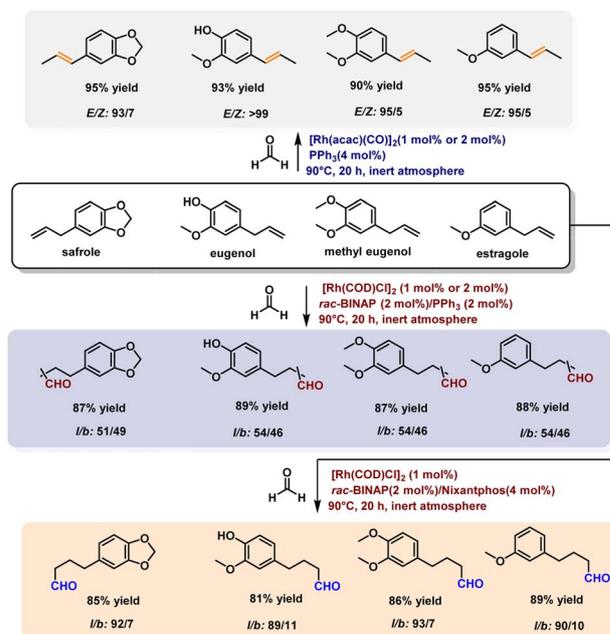

Fig. 4 Rh-catalyzed transfer hydroformylation of biobased olefins with formaldehyde.

Beyond broadening the substrate scope of formaldehyde-mediated hydroformylation, in-depth mechanistic investigations are equally crucial for the catalytic system. In 2016, Rosales and co-workers investigated the kinetics and mechanism of formaldehyde-mediated hydroformylation of alkanes catalyzed by a cationic bis(diphosphine)rhodium complex[21] (Fig. 5). They employed acetylacetonate (acac) as a precatalyst to elucidate the mechanism of 1-hexene hydroformylation with formaldehyde via experimental kinetics, coordination chemistry studies as well as DFT calculations. They found that the reaction proceeds via a hydroacylation pathway, rather than the conventional mechanism in which formaldehyde decomposes into CO and H_2 prior to hydroformylation. During the catalytic cycle, formaldehyde first undergoes oxidative addition to the rhodium center, forming the active intermediate $[Rh(H)(CHO)(\kappa^2\text{-}P,P\text{-}dppe)_2]^+$ (dppe: 1,2-bis(diphenylphosphino)ethane). Subsequently, the olefin inserts into the Rh–H bond, which was identified as the rate-determining step (RDS). Finally, reductive elimination yields the aldehyde product and regenerates the active catalyst species. DFT calculations revealed that the activation barrier for the hydroacylation pathway is approximately 31.5 kcal mol^{-1}, whereas the classical pathway involving in situ syngas generation from formaldehyde exhibits a higher barrier of about 36.5 kcal mol^{-1}. Therefore, the hydroacylation route is both thermodynamically and kinetically more favorable. Furthermore, experimental results showed that under $[Rh(\kappa^2\text{-}P,P\text{-}dppe)_2]acac$ catalysis, the hydroformylation of 1-hexene with formaldehyde proceeds significantly faster than the corresponding reaction performed under low-pressure syngas (Table 1), further confirming the efficiency of this CO-free hydroformylation mechanism.

Formic acid as carbonyl source

Formic acid (FA) is an important bulk chemical that has been widely recognized as a sustainable and environmentally benign energy carrier, capable of delivering H_2 through dehydrogenation[22] or CO via decarbonylation.[23] Given that formic acid can decompose to CO under suitable catalytic conditions, it has emerged as an ideal carbonyl source for the carbonylation of

Table 1 The rate of 1-hexene hydroformylation with formaldehyde and syngas[a]

Carbonyl source	$10^5 \, r_i$/M s^{-1}
Formaldehyde	9.90 ± 0.40
3 atm syngas	5.18 ± 0.11

[a] Conditions: [Rh] = 1.68 mM, [1-hexene] = 0.50 M, [CH_2O] = 0.22 M; solvent: 1,4-dioxane; total volume = 30 mL, T = 373 K. r_i: initial rates of the reaction.

alkenes, alkynes, and related substrates. In the past decade, formic acid-based catalytic systems have been extended to a variety of transformations, such as hydroformylation, esterification, carboxylation, and have achieved significant advances.[24] In this section, we will focus on formic acid-mediated hydroformylation.

A serious of innovations in hydroformylation by employing formic acid as the carbonyl source was pioneered by Shi and co-workers. In 2016, they reported a highly regioselective, Pd-catalyzed hydroformylation process of olefins using formic acid combined with acetic anhydride (Ac_2O) as a CO surrogate[25] (Fig. 6). Using a $Pd(OAc)_2$/dppp (1,3-bis(diphenylphosphino) propane) catalyst in the presence of Bu_4NI, styrene and a wide range of aryl or alkyl terminal alkenes were hydroformylated to afford linear aldehydes in up to 93% yield, with $l:b$ ratios over 20:1. Crucially, both the bite angle of the bidentate phosphine ligand and iodide additive decided the selectivity toward this reaction. Primary alcohols play a crucial role in the field of organic synthesis, pharmaceuticals, fine chemicals, and materials. Building on aforementioned catalytic strategy, this team implemented a tandem hydroformylation–reduction sequence to efficiently synthesize primary alcohols in 2025 (ref. 26) (Fig. 6). In this case, the aldehydes generated via $Pd(OAc)_2$/dppp
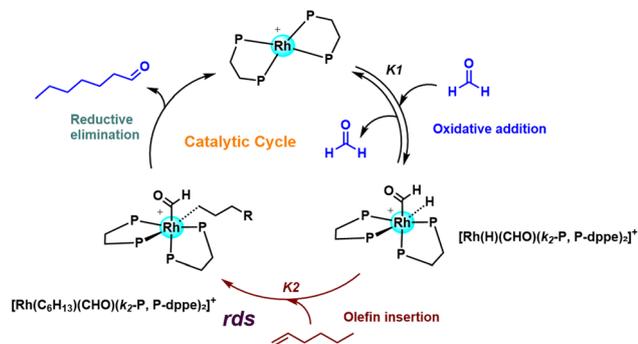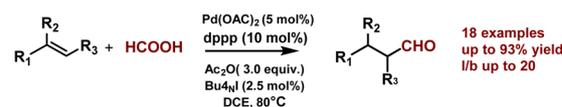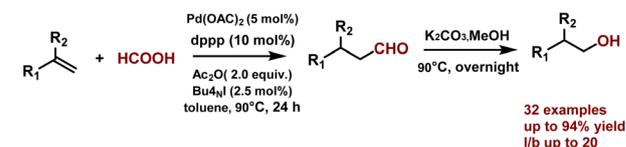

Fig. 5 Catalytic cycle for the hydroformylation of olefine with formaldehyde catalyzed by $[Rh(\kappa^2\text{-}P,P\text{-}dppe)_2]acac$.
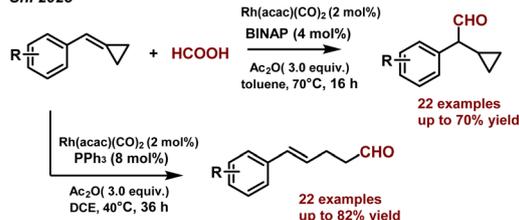

Fig. 6 Rh and Pd-catalyzed hydroformylation of alkyl terminal olefins, vinyl arenes and benzylidenecyclopropanes with HCOOH.

catalysis were subsequently treated with K_2CO_3 and methanol, affording a wide range of primary alcohols with yields reaching up to 94% and selectivity ratios as high as 20 : 1. To broaden the substrate scope, they developed a series of highly efficient and regioselective hydroformylation processes catalyzed by either Pd or Rh, employing HCO_2Na/Ac_2O or HCO_2H/Ac_2O as the carbonyl source.[27] The linear aldehydes can be obtained in good yields with high l/b ratios. Each catalytic strategy presented unique advantages: the Pd-catalyzed protocol demonstrated outstanding regioselectivity for vinyl arenes, while the Rh-catalyzed reaction showed superior performance with certain alkyl terminal olefins. Recently, Shi's team expanded their study to highly strained small-ring compounds, using benzylidene-cyclopropanes as model substrates for the Rh-catalyzed hydro-formylation reaction employing formic acid as the carbonyl source.[28] Under the optimized $Rh(acac)(CO)_2/HCO_2H/Ac_2O$ system, the reaction pathway was found to be strongly depen-dent on the ligand employed. When PPh_3 was used as the ligand, the reaction selectively produced ring-opened γ,δ-unsaturated aldehydes in up to 82% yield with excellent *trans*-selectivity, whereas the use of BINAP favored the formation of ring-retained 2-cyclopropyl-2-arylacetaldehydes, achieving yields of up to 70%. The reaction exhibited broad substrate scope, tolerating various aryl and heteroaryl substituents, and proceeded efficiently under mild conditions (40 or 70 °C) without the need for high-pressure CO or H_2. Mechanistic investigations suggested that the Rh–H species originated from the decomposition of formic acid, and the transformation could proceed through two competing pathways-β-C elimination or migratory insertion with the electronic and steric properties of the ligand playing a decisive role in determining product selectivity.

In 2021, Liu and co-workers have achieved notable advance in the decomposition of formic acid into syngas, an essential process for Rh-catalyzed olefin hydroformylation[29] (Fig. 7). In this case, the authors demonstrated that, under the $Rh(acac)(CO)_2/Xantphos$ catalytic system, formic–acetic anhydride (AFA) upon FA reacting with Ac_2O was effectively promoted to release CO *in situ* while the free *cis*-FA monomer acts as a hydride donor to liberate H_2 and generate the active Rh–H species responsible for the high hydroformylation effi-ciency. In terms of substrate scope, the protocol exceled with both aryl and aliphatic olefins. A range of substituted styrenes afforded the desired aldehydes with 92–98% conversion and 93–97% selectivity. As for alkyl terminal olefins, still delivered linear aldehydes in 92% yield, despite a modest l/b ratio ($\sim$0.4) due to steric effects. Internal olefins predominantly yielded branched aldehydes.

Transitioning from petrochemical to bio-renewable feed-stocks has emerged as an undeniable imperative.[30] As potential bioresources, terpenes and propenylbenzenes play significant roles in the fragrance, cosmetics, and pharmaceutical sectors.[31,32] Similarly, Delolo's team also developed a hydro-formylation process of renewable terpenes and propenylbenz-enes based on the $Rh(acac)(CO)_2/Xantphos$ catalytic system with a mixture of formic acid (FA) and acetic anhydride (Ac_2O)[33] (Fig. 8). When estragole was employed as the model substrate, the authors obtained an 93% conversion and 92% aldehyde selectivity. Importantly, they demonstrated that conducting the reaction in the green solvent 2-MeTHF achieved performance comparable to that in conventional THF, while providing
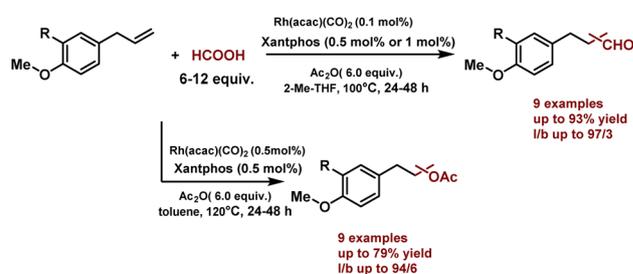
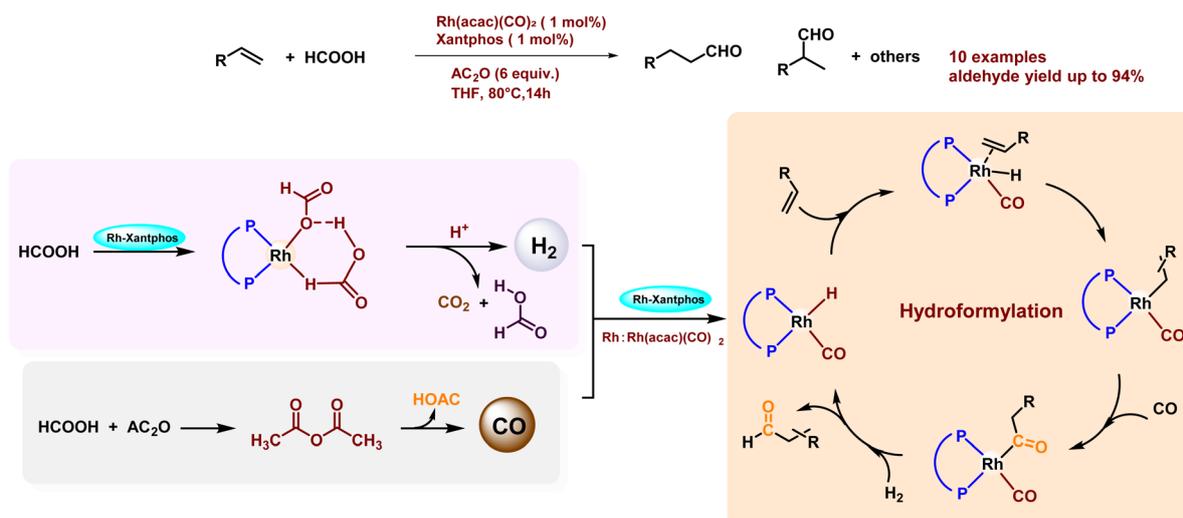**Fig. 8** [Rh–Xantphos]-catalyzed hydroformylation of olefins with HCOOH.

Fig. 7 The proposed catalytic mechanism over $Rh(acac)(CO)_2$–Xantphos for the hydroformylation of olefins with HCOOH.

superior environmental benefits. In addition, they performed the consecutive hydrogenation of the aldehyde, followed by *O*-acetylation, which formally introduced a methyl acetate moiety across the C–C double bond in a tandem process. This strategy employed a one-pot approach to accomplish a process that conventionally requires three separate steps under syngas conditions, thereby significantly streamlining the procedure.

Beyond using olefins as model substrates, Zhou and Ding reported the Rh-catalyzed hydroformylation of alkynes with formic acid as the CO surrogate[34] (Fig. 9). Xantphos was once again screened as the optimal ligand, which was attributed to its large bite angle when complexing with rhodium. This catalytic system was suitable for aryl, heteroaryl, and alkyl alkynes; however, terminal alkynes exhibited poor reactivity and mainly produced hydrogenation byproducts.

Most reported hydroformylation reactions employing formic acid as a carbonyl source have been carried out in homogeneous catalytic systems, which often suffer from challenging catalyst separation and limited recyclability, particularly in the transformation of higher olefins. In 2026, Wu and co-workers pioneered the development of a palladium(II) single-site solid catalyst (Pd(II)–MOF-808) based on a metal organic framework (MOF) architecture and successfully applied it to the formic acid-driven carbonylation of styrene (Fig. 10). The open metal sites within MOF-808 not only stabilized and anchored isolated Pd(II) centers but also allowed functionalization through the introduction of phosphine ligands, thereby forming highly active Pd(II) coordination species. Under mild conditions (80 °C, 24 h), Pd(II)–MOF-808 incorporating dppp afforded 3-phenyl-propanal with a 73% yield and > 99% selectivity, while Pd(II)–PPh$_3$–MOF-808 achieved a 49% yield of 3-phenylpropanoic acid after 18 h at 80 °C. DFT calculations further demonstrated that the nucleophilicity and geometric characteristics of the ligand play a decisive role in determining product distribution which ligands with higher nucleophilicity favored aldehyde formation, whereas less nucleophilic ligands tend to promote the formation of carboxylic acids.

CO$_2$/H$_2$ as carbonyl source

Carbon dioxide, a major component of greenhouse gases, presents an urgent scientific challenge: the valorization of this abundant waste into a viable energy feedstock. Despite its
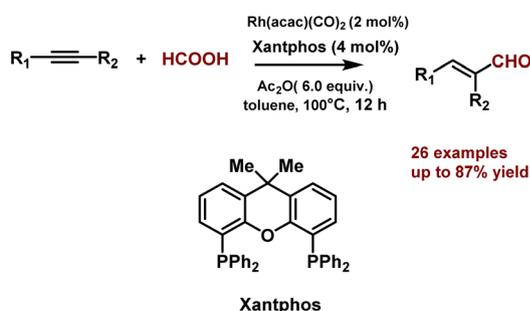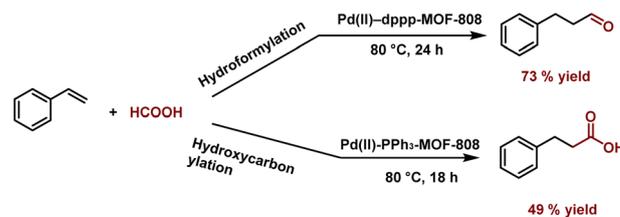

Fig. 10 [Pd(II)–MOF-808]-catalyzed hydroformylation and hydroxycarbonylation styrene of with HCOOH.

pronounced thermodynamic and kinetic stability, chemists continue to pursue its conversion into high-value products.[35] Among these efforts, the most extensively investigated strategy involves employing CO$_2$ as a CO surrogate in olefin carbonylation reactions. The general strategy is to reduce CO$_2$ *in situ* to CO, which subsequently participates in carbonylation processes. Usually, this part of studies was involved gas–liquid reaction. The crucial step in this transformation is the reverse water–gas shift reaction (RWGS).[36] In this section, we summarize recent advances in olefin hydroformylation reactions employing CO$_2$/H$_2$ as the carbonyl source.

In 2000, Tominaga *et al.* reported a Ru-catalyzed hydroformylation involving CO$_2$, H$_2$, and olefins[37] (Fig. 11). In this sequence, CO$_2$ is first converted to CO *via* the RWGS reaction, the generated CO then undergoes carbonylation with the olefin to produce an aldehyde, which is subsequently hydrogenated by H$_2$ to yield the corresponding alcohol. Using H$_4$Ru$_4$(CO)$_{12}$ as the catalyst and LiCl as the additive, an 88% yield of cyclohexylmethanol and a 3% yield of cyclohexyl formaldehyde were obtained from cyclohexene. Detailed studies revealed that the identity of the halide additive exerted a significant influence on catalytic performance (I$^-$ < Br$^-$ < Cl$^-$), which correlated with their relative proton affinities.

While the catalytic carbonylation of olefins with CO$_2$ to yield carboxylic acids, esters, and alcohols have been increasingly reported, the strong reducing ability of ruthenium catalysts and the high temperatures required for rhodium catalysis both precluded the formation of aldehyde. In 2016, Ding and co-workers reported the first method for the synthesis of aldehydes from alkenes and CO$_2$/H$_2$, without formation of the corresponding alcohols[38] (Fig. 10). They screened the Rh(acac)(CO)$_2$/bis(phosphoramidite) as the optimal catalytic system, employing poly(methylhydrosiloxane) (PMHS) as an effective reductant for CO$_2$ transformation, which afforded aldehydes in yield of up to 70% with regioselectivities reaching 9 : 1 (*l*/*b*). A turnover number (TON) of up to 1 000 000 was


Fig. 9 [Rh–Xantphos]-catalyzed hydroformylation of alkyne with HCOOH.

Fig. 11 Ruthenium-catalyzed hydroformylation/reduction of cyclohexene with carbon dioxide.

RSC Advances

achieved after 12 hours, while maintaining excellent selectivity for linear aldehydes. Similarly, He and co-workers developed a Cu/Co tandem catalytic protocol to perform the hydroformylation of olefins using CO_2/H_2, with PMHS also serving as a reductant[39] (Fig. 12). This protocol was implemented *via* two steps: the Cu-catalyzed reduction of CO_2 by PMHS, followed by co-catalyzed hydroformylation. Both terminal and internal olefins were successfully converted to their corresponding aldehydes in moderate to excellent yields. They proposed that maintaining a sufficiently high *in situ* CO partial pressure was essential for effective hydroformylation, and that triphos oxide significantly enhanced both $HCo(CO)_4$ formation and CO migratory insertion. Compared to the high cost of rhodium, the use of cobalt is far more economical.

To accelerate the industrialization of CO_2-based carbonylation and streamline downstream separation, Beller and co-workers developed a "two-chamber system" process to generated CO on demand and immediately consumed it[40] (Fig. 13). They designed a novel heterogeneous copper $10Cu@SiO_2$–PHM catalyst, which in a continuous mode converted CO_2 into CO *via* the RWGS reaction with nearly 100% CO selectivity and a 27% CO_2 conversion. Bypassing the need for separation, purification, or removal of water and residual CO_2, the generated CO can be fed directly into a variety of industrially and synthetically valuable carbonylation reactions including olefin hydroformylation, alkyne methoxycarbonylation, and aryl-halide aminocarbonylation, thereby this process substantially improved the safety and integration. In the case of olefin hydroformylation, the $Rh(acac)(CO)_2$/6-DPPon (6-(diphenylphosphino)-2(1H)-pyridinone) catalytic system delivered linear aldehyde yields exceeding 90% and a linear-to-branched (*l*/*b*) ratio greater than 99 : 1 when using 1-octene and 1-decene as substrates. By converting CO_2/H_2 into "safe" CO and consuming it *in situ*, this approach not only reduced the risks associated with CO storage and transport but also served as a scalable "mini-factory" facilitating scale-up and continuous production.
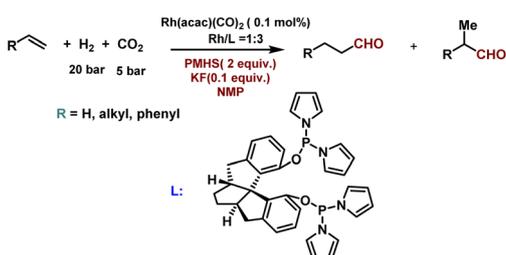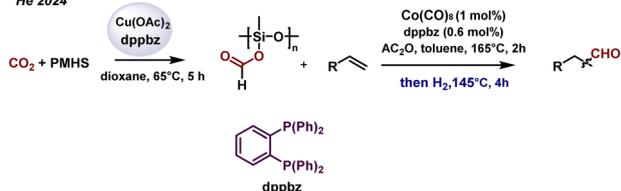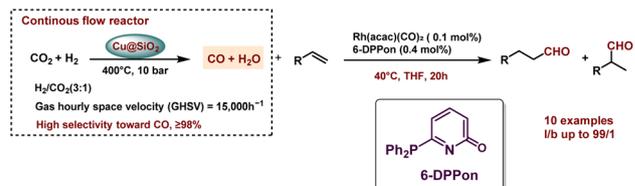

Fig. 13 Selective copper-catalyzed CO generation from CO_2 and direct utilization in hydroformylation reaction.

The preceding section reviews several efficient alkene hydroformylation strategies with formic acid as the carbonyl source. Typically, formic acid is generated *via* catalytic hydrogenation of CO_2. In 2021, Sun and co-workers developed a bifunctional Rh/PTA (1,3,5-triaza-7-phosphaadamantane) catalytic system *via in situ* generation of formic acid from CO_2 (ref. 41) (Fig. 14). The Rh/PTA system concurrently facilitated CO_2 hydrogenation and alkene hydroformylation, achieving efficient and selective conversion of alkenes using a CO_2/H_2 mixture as a syngas surrogate. In this case, the desired aldehydes can be obtained in up to 97% yield with 93/7 regioselectivity. Notably, the activity and regioselectivity of bidentate ligands were inferior to monodentate PTA, which might be attributed to its built-in basic site and tris-chelated mode.

Recently, efforts in this field have switched from homogeneous to heterogeneous catalysis. Sadeghzadeh and co-workers reported the synthesis of multi-site ionic liquids immobilized on dendritic fibrous nanosilica (DFNS–IL) in an aqueous medium, followed by uniform loading of ruthenium nanoparticles to yield DFNS–IL@Ru[42] (Fig. 15). Under mild conditions (90 °C, 10 h), this nanocatalyst employs a CO_2/H_2 mixture as a syngas surrogate, delivering excellent catalytic performance with aldehyde isolated yields up to 96% from various terminal alkenes. Recycling studies demonstrated only a 4% drop in yield after 10th runs. The DFNS–IL@Ru catalyst fully exemplified green chemistry principles and offered a versatile platform for developing other highly efficient nanocatalysts.

To address the limited regioselectivity of monophosphine ligand and the structural complexity and high cost of diphosphine ligands, Ding and co-workers introduced an innovative synergistic strategy employing two monophosphine species[43] (Fig. 16). A concise and efficient copolymerization method was developed to co-polymerize v-PPO (1,1′-((4-vinylphenoxy)phosphanediyl)bis(1H-pyrrole)) and PPh_3, yielding a porous organic polymer (POL–PPO&PPh_3). And single-atom Rh was dispersed in this polymer, affording the single-atom catalyst (Rh–POL–PPO&PPh_3). Under CO_2/H_2 conditions, this catalyst achieved highly efficient olefin hydroformylation,

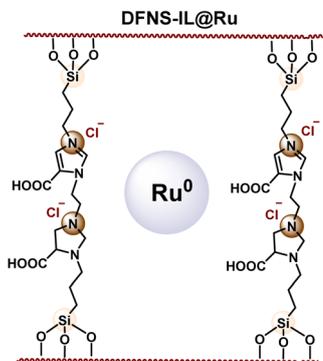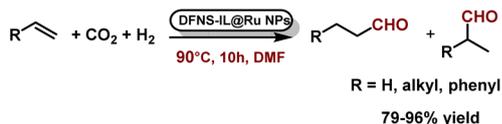**Fig. 12** PMHS-promoted hydroformylation of olefins with CO_2/H_2.
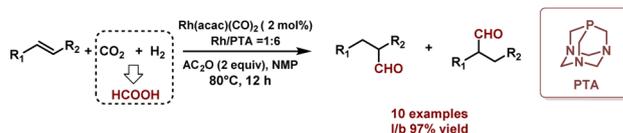
Fig. 14 Rh–PTA-catalyzed hydroformylation of olefins with CO_2/H_2.

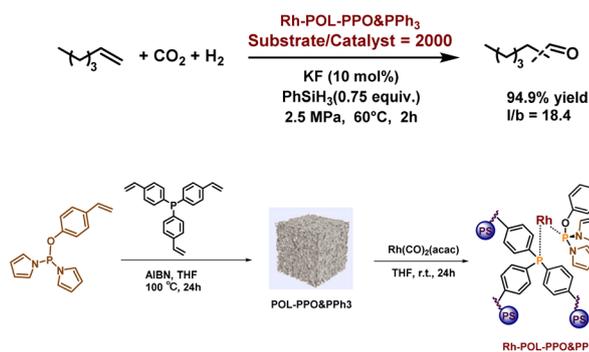**Fig. 15** DFNS–IL@Ru-catalyzed hydroformylation of olefins with CO_2/H_2.

Fig. 16 Rh–POL–PPO&PPh$_3$-catalyzed hydroformylation of olefins with CO_2/H_2.

exhibiting outstanding regioselectivity (linear/branched ratio up to 18.4) and excellent activity (conversion up to 94.9%), outperforming traditional monophosphine systems and rivaling the diphosphine frameworks. DFT calculations revealed that the synergistic interaction between the two monophosphine ligands promoted the coordination of Rh at the terminal olefin carbon, favoring linear aldehyde formation. However, this strategy was limited to aliphatic alkenes. In 2025, the team further advanced this research by doping nitrogen sites near the Rh–P active centers[44] (Fig. 17). The resulting Rh$_1$/POPs–P&N catalyst generated more active species *in situ*, thereby enhancing substrate conversion efficiency, particularly in the case of Rh$_1$/POPs–PPh$_3$&PMPD (MDP: *m*-phenyl-enediamine). The catalytic system exhibited a broad substrate scope, efficiently converting twelve olefins-including aromatic alkenes, affording aldehyde yields up to 89% with a linear-to-branched ratio of 13.1. The catalyst retained full activity over five consecutive cycles, indicating excellent stability.

Similarly, Shi and co-workers also reported a single-atom catalytic hydroformylation in 2024.[45] They developed a novel
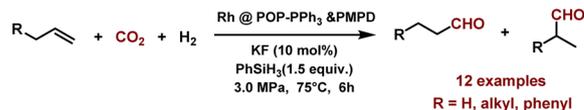

Fig. 17 Rh–POL–PPO–PPh$_3$&PMPD-catalyzed hydroformylation of olefins with CO_2/H_2.

heterogeneous rhodium catalyst encapsulated with bisphosphine-ligand, synthesized *via* free-radical copolymerization of diphosphine monomers fully complexed with Rh with 3v-PPh$_3$ (Fig. 18). Aromatic and aliphatic alkenes with different functional groups were smoothly converted into aldehydes with 58–89% yield. The high activity and stability of the catalyst were attributed to the abundant but dispersed phosphine ligand inside the pore path and the strong coordination between Rh and the bisphosphine ligand. Notably, although this work closely parallels the study of Ding's group, it differs in its ligand-copolymerization strategy and substrate scope.

In the past few years, electrocatalysis plays a crucial role in the field of carbon dioxide reduction, and several studies have already reported using CO and H$_2$ generated by electrocatalytic CO$_2$ reduction to drive hydroformylation reactions. For example, Li and He reported the cascade electrocatalytic and thermocatalytic reduction of CO$_2$ to propionaldehyde[46] (Fig. 19). Using Cu(OH)$_2$ nanowires as a precatalyst, CO$_2$/H$_2$O was electrochemically reduced to concentrated C$_2$H$_4$, CO, and H$_2$ gases in a zero-gap membrane electrode assembly (MEA) reactor. Subsequently, hydroformylation reaction was investigated with a series of rhodium–phosphine complexes, screening Rh–DPPB (1,4-bis(diphenylphosphino)butane) as the optimal catalyst, achieving a propionaldehyde selectivity of 37.7% and a total C$_3$ oxygenate selectivity of 44.1%, and the dppb ligand exhibited the highest activity with a TON of 1148. This system represents the first efficient coupling of CO$_2$ electroreduction products (C$_2$H$_4$/CO/H$_2$) with thermal hydroformylation, enabling the sustainable synthesis of C$_3$ chemicals directly from CO$_2$.
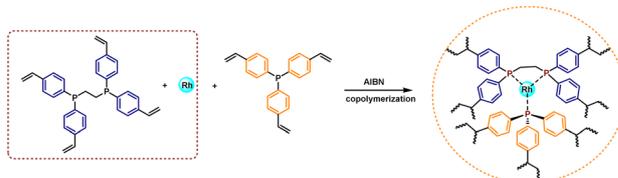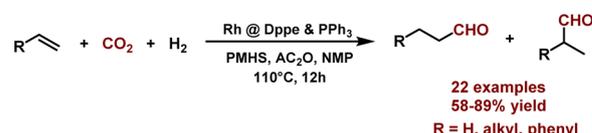

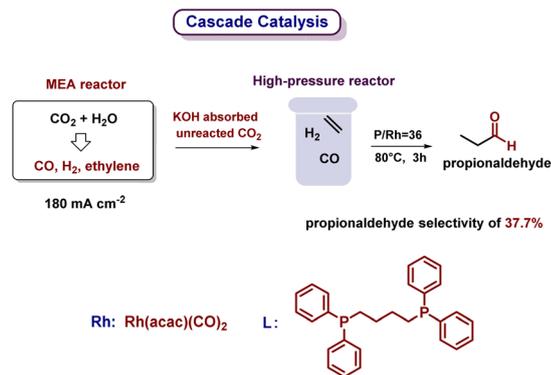**Fig. 18** Rh@dppe&PPh$_3$-catalyzed hydroformylation of olefins with CO_2/H_2.

Fig. 19 Electrocatalytic and thermocatalytic CO_2 reduction to propionaldehyde.

Fig. 21 Tandem electrocatalysis and hydroformylation of phenylacetylene with CO_2.

Later, Liu and co-workers generated syngas *in situ* through electrochemical CO_2 reduction (CO_2RR) and directly converted CO_2 and olefins into aldehydes using a typical Rh catalytic system, achieving a "one-step" green synthesis of bulk chemicals from an environmental burden[47] (Fig. 20). In their study, a "vial-in-vial" reactor was employed to achieve spatial separation of the CO_2RR and hydroformylation zones, while allowing CO and H_2 to freely diffused between the two compartments, effectively preventing catalyst interference. Under these conditions, the conversion of styrene to aldehydes reached a yield of up to 97%, and the linear-to-branched aldehyde ratio was comparable to those reported under classical pressurized conditions. This work innovatively transformed the undesired hydrogen evolution (HER) byproduct from CO_2RR into a valuable hydrogen source and proposed a new paradigm of spatial separation strategy, providing an effective approach to overcome incompatibility issues in multi-catalyst systems.

Similarly, based on an electrochemical strategy, Xu's group developed a tandem electrocatalytic hydroformylation system that directly converts CO_2 into high-carbon aldehydes using alkynes as substrates[48] (Fig. 21). The designed Ni_xCo_{1-x}@NCNT electrocatalysts were capable of converting CO_2 and H_2O into syngas with nearly 100% total faradaic efficiency under industrial-level current densities. By tuning the Ni/Co ratio and current density, the H_2/CO ratio could be precisely adjusted within a wide range of 0–5.3, allowing flexible control of syngas composition. Among them, $Ni_{0.20}Co_{0.80}$@NCNT produced syngas with an H_2/CO ratio of approximately 1.6, ideally matching the requirements of the downstream Rh–indolyl biphosphoramidite ligand catalytic system. This tandem process achieved a phenylacetylene conversion of 87% and an aldehyde
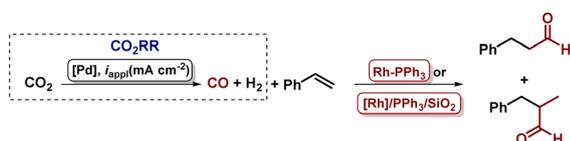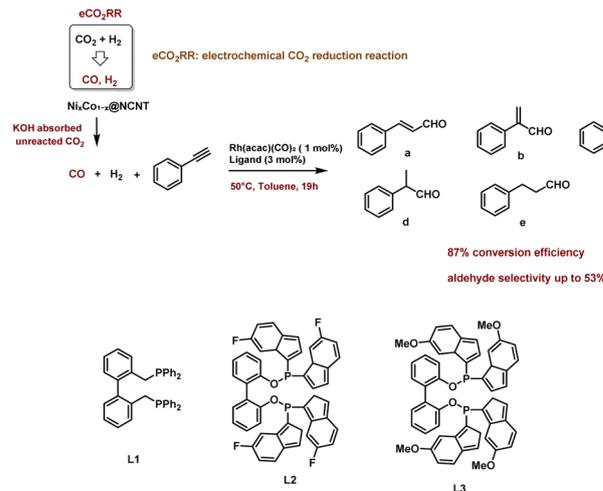
selectivity of 53% at room temperature, enabling the efficient synthesis of high-carbon aldehydes from CO_2. Distinct from Liu's spatially separated configuration, this work featured a continuous gas–liquid two-phase reaction process and further broadened the substrate scope to alkynes. It establishes a highly efficient and scalable CO_2 conversion pathway, offering a new paradigm for the design of multi-step tandem reactions driven by electrocatalysis.

With the rapid advancement of artificial intelligence (AI), high-throughput screening (HTS) and Bayesian optimization have shown significant potential in accelerating catalyst development, though their applications have largely been limited to atmospheric-pressure systems. Fujitani and Tanabe established a closed-loop high-throughput optimization platform that integrated AI and robotic operation, using the direct hydroformylation of CO_2 as a model reaction.[49] By implementing a transfer-learning-based surrogate model, the system efficiently identified optimal reaction conditions within a short period. Under conditions employing small amounts of Rh and Ru bimetallic catalysts in combination with an ionic liquid containing chloride anions, the aldehyde yield was enhanced by 1.5-fold relative to the previously reported benchmark. The corresponding codes, models, and initial datasets have been made publicly available on GitHub (**https://github.com/HirokiSugisawa/BBO**), offering an extensible framework for future research.

The three alternative carbonyl sources exhibit distinct features. Formaldehyde enables relatively mild conditions, releasing syngas at moderate temperatures without high pressure or additional additives. It shows high activity and favorable *l/b* ratios for terminal olefins, along with excellent linear selectivity toward aromatic substrates such as styrene. Formic acid is safe, inexpensive, and renewable, and achieves notable linear selectivity in aromatic olefins. However, it typically requires additives (*e.g.*, acetic anhydride, iodides) to promote CO release, generating byproducts such as acetic acid, while its selectivity decreases with internal or branched olefins.CO_2,

Fig. 20 Integrated electrochemical CO_2 reduction and aromatic alkenes hydroformylation with Rh catalyst in a vial-in-vial reactor.

though thermodynamically stable, represents the most sustainable option. It must first undergo the reverse water–gas shift (RWGS) reaction to form CO, which raises the demands on catalytic systems. Despite the need for high H_2 consumption and multifunctional catalysts, CO_2 offers advantages of safety, low cost, non-toxicity, and facile catalyst recovery. With optimization, some systems can achieve linear selectivity comparable to syngas processes ($l/b > 99:1$), though substrate scope remains limited.

Summary and outlook

In conclusion, investigations into hydroformylation using formaldehyde, formic acid, and carbon dioxide as carbon monoxide surrogates have demonstrated the immense potential of these alternative C_1 sources. By eliminating the need to handle toxic CO gas, these strategies allow reactions to proceed under milder and inherently safer conditions, in turn spurring the development of diverse and innovative catalytic platforms. While Rh and Co catalysts remain predominant in both industrial and academic hydroformylation, recent studies show that alternative metals such as Pd and Ru can also serve as effective catalysts in carbonyl surrogate systems.

Notably, each carbonyl surrogate exhibits distinct reactivity features that can be leveraged to influence product selectivity and reaction conditions. As shown in Table 2, the advantages and limitations of the three carbonyl surrogates are systematically summary. Formaldehyde, for instance, usually acts as an *in situ* syngas source under relatively mild conditions (moderate temperatures, without high pressure or added promoters). In such systems, Rh(ɪ)/bidentate phosphine ligands (*e.g.*, BINAP, Xantphos, Ph–BPE) effectively promote linear or asymmetric hydroformylation, providing high catalytic activity and a strong preference for linear aldehyde formation (*i.e.*, high l/b ratios) in terminal alkenes and aromatic substrates such as styrene. Formic acid is another safe, inexpensive, and renewable

carbonyl surrogate that likewise tends to favor linear selectivity in aromatic olefins. These reactions typically rely on Pd or Rh complexes supported by bidentate phosphine ligands such as dppp or Xantphos, and in recent years, the strategy has been extended to heterogeneous architectures to enhance catalyst recyclability under acidic conditions, such as Pd(ɪɪ)–MOF catalyst. However, formic acid systems usually require additives (*e.g.*, acetic anhydride or iodide salts) to release CO, which leads to byproduct formation (*e.g.*, acetic acid), and their selectivity advantage diminishes when applied to internal or branched olefins. Carbon dioxide is arguably the most sustainable carbonyl source, albeit the most inert. It must first be converted (for example, *via* a reverse water–gas shift step with H_2) to generate CO, a requirement that entails high reductant consumption and robust, multifunctional catalysts (*e.g.*, Rh, Ru, or Co). Nevertheless, CO_2 is non-toxic, abundant, and low-cost. In some optimized systems, it can deliver nearly exclusive linear product formation ($l/b > 99:1$), although so far only for a limited range of substrates.

Interestingly, the use of carbonyl surrogates can unlock unconventional reaction pathways. For instance, in a CO_2/Rh–PTA system, hydroformylation proceeds *via* a formate (HCOOAc) intermediate instead of the usual direct CO insertion, yielding predominantly linear aldehydes with superior regioselectivity compared to the traditional pathway.[41] This mechanistic nuance underscores how deploying carbonyl surrogates offers new opportunities to control regio- and stereoselectivity beyond what is achievable with classical syngas.

Despite these advances, several challenges remain for carbonyl surrogate-based hydroformylation. For example, formaldehyde-driven systems often use paraformaldehyde or aqueous formalin as the feedstock with Rh–phosphine catalysts; the high-water content (>50%) in formalin may adversely affect catalyst stability and recyclability, yet this impact has not been fully elucidated. Introducing water-tolerant (*e.g.*, ionic) phosphine ligands or

Table 2 Comparative analysis of three carbonyl sources

	Advantages	Limitations
HCHO	(1) Mild, safe, and easy to operate	(1) High water content in formaldehyde may cause catalyst deactivation or hinder recyclability
	(2) Excellent linear selectivity for terminal and aromatic alkenes (*e.g.*, styrene)	(2) Limited applicability to branched or functionalized alkenes
	(3) Applicable to asymmetric hydroformylation	
HCOOH	(1) Low-cost, mild, safe, renewable, green	(1) Additives needed for CO release (*e.g.*, Ac_2O, I^-)
	(2) Excellent linear selectivity for aromatic terminal alkenes	(2) Byproducts (*e.g.*, acetic acid)
	(3) Compatible with renewable substrates (*e.g.*, terpenes, allylbenzene)	(3) Catalyst aggregation under acidic conditions
		(4) Lower selectivity for internal or branched alkenes
CO_2/H_2	(1) Abundant, non-toxic, green and sustainable	(1) Requiring high temperature/pressure or external reductants (PMHS, H_2)
	(2) Excellent linear selectivity for several alkenes and alkynes	(2) Complex catalytic systems (multi-functional or bimetallic catalysts)
		(3) Limited substrate scope

utilizing anhydrous formaldehyde sources (such as methanol-stabilized formaldehyde solutions) could help mitigate this issue. In formic acid-based systems, the strongly acidic reaction environment can promote metal catalyst aggregation, compromising catalyst longevity and activity. More generally, many carbonyl surrogate approaches suffer from relatively low catalytic efficiency and a limited substrate scope, making them less competitive than conventional syngas-based hydroformylation. Even systems that achieve high yields with simple linear alkenes tend to exhibit sharply reduced conversion or selectivity when substrates bear complex functional groups or significant steric hindrance.

To fully harness the potential of carbonyl surrogates in hydroformylation, the development of more active, selective, and robust catalytic systems is essential. In particular, advancing CO_2-based hydroformylation is highly significant: if CO_2—one of the major greenhouse gases—can be efficiently utilized as a carbonyl source for producing value-added aldehydes, it would reduce reliance on fossil-derived syngas and could potentially surpass traditional processes in both economic viability and environmental sustainability. With continued innovation in catalyst design and process optimization, carbonyl surrogate strategies may not only match the efficacy of classical syngas hydroformylation but also offer greener and more versatile routes to fine chemicals and complex molecules.

Author contributions

Z.-R. Z. conceived the idea and wrote the paper, S. L., W.-R. F., X.-Y. W., H.-C. L., H. C., L. W., F.-J. Z., and S.-B. F. referred to the literatures and reviewed the paper.

Conflicts of interest

There are no conflicts to declare.

Data availability

No primary research results, software or code have been included and no new data were generated or analysed as part of this review.

Acknowledgements

Notes and references

1 R. Franke, D. Selent and A. Börner, *Chem. Rev.*, 2012, **112**, 5675–5732.
2 D. Gorbunov, M. Nenasheva, G. Shashkin, V. Shapovalov, P. Shvets, E. Naranov, A. Maximov, A. Guda and A. Soldatov, *J. Ind. Eng. Chem.*, 2024, **136**, 46–72.
3 B. Zhang, D. Peña Fuentes and A. Börner, *ChemTexts*, 2021, **8**, 2.
4 T. Morimoto and K. Kakiuchi, *Angew. Chem., Int. Ed.*, 2004, **43**, 5580–5588.
5 A. Bonde, J. B. Jakobsen, A. Ahrens, W. Huang, R. Jackstell, M. Beller and T. Skrydstrup, *Chem*, 2025, **11**, 102494.
6 T. Okano, T. Kobayashi, H. Konishi and J. Kiji, *Tetrahedron Lett.*, 1982, **23**, 4967–4968.
7 M. Rosales, A. González, B. González, C. Moratinos, H. Pérez, J. Urdaneta and R. A. Sánchez-Delgado, *J. Organomet. Chem.*, 2005, **690**, 3095–3098.
8 M. Rosales, F. Arrieta, P. Baricelli, Á. González, B. González, Y. Guerrero, C. Moratinos, I. Pacheco, H. Pérez and J. Urdaneta, *Catal. Lett.*, 2008, **126**, 367–370.
9 G. Makado, T. Morimoto, Y. Sugimoto, K. Tsutsumi, N. Kagawa and K. Kakiuchi, *Adv. Synth. Catal.*, 2010, **352**, 299–304.
10 M. Taddei, E. Cini, E. Airiau, N. Girard, A. Mann and J. Salvadori, *Synlett*, 2010, **2011**, 199–202.
11 M. Uhlemann, S. Doerfelt and A. Börner, *Tetrahedron Lett.*, 2013, **54**, 2209–2211.
12 T. Yu, Z. Ding, W. Nie, J. Jiao, H. Zhang, Q. Zhang, C. Xue, X. Duan, Y. M. A. Yamada and P. Li, *Chem.–Eur. J.*, 2020, **26**, 5729–5747.
13 J. García-Lacuna, T. Fleiß, R. Munday, K. Leslie, A. O'Kearney-McMullan, C. A. Hone and C. O. Kappe, *Org. Process Res. Dev.*, 2021, **25**, 947–959.
14 T. Morimoto, T. Fujii, K. Miyoshi, G. Makado, H. Tanimoto, Y. Nishiyama and K. Kakiuchi, *Org. Biomol. Chem.*, 2015, **13**, 4632–4636.
15 J. A. Fuentes, R. Pittaway and M. L. Clarke, *Chemistry*, 2015, **21**, 10645–10649.
16 R. Pittaway, P. Dingwall, J. A. Fuentes and M. L. Clarke, *Adv. Synth. Catal.*, 2019, **361**, 4334–4341.
17 M. Vilches-Herrera, M. Concha-Puelles, N. Carvajal, J. Molina, R. Santander, M. Caroli Rezende and S. Lühr, *Catal. Commun.*, 2018, **116**, 62–66.
18 L. A. Pfaltzgraff and J. H. Clark, in *Advances in Biorefineries*, ed. K. Waldron, Woodhead Publishing, 2014, pp. 3–33, DOI: **10.1533/9780857097385.1.3**.
19 C. Chapuis and D. Jacoby, *Appl. Catal., A*, 2001, **221**, 93–117.
20 M. Concha-Puelles, A. Cortínez, N. Lezana, M. Vilches-Herrera and S. Lühr, *Catal. Sci. Technol.*, 2022, **12**, 6883–6890.
21 M. Rosales, H. Pérez, F. Arrieta, R. Izquierdo, C. Moratinos and P. J. Baricelli, *J. Mol. Catal. A: Chem.*, 2016, **421**, 122–130.
22 S. Kar, M. Rauch, G. Leitus, Y. Ben-David and D. Milstein, *Nat. Catal.*, 2021, **4**, 193–201.
23 J.-P. Simonato, *J. Mol. Catal. A: Chem.*, 2003, **197**, 61–64.
24 J. Cao, Z.-J. Zheng, Z. Xu and L.-W. Xu, *Coord. Chem. Rev.*, 2017, **336**, 43–53.
25 W. Ren, W. Chang, J. Dai, Y. Shi, J. Li and Y. Shi, *J. Am. Chem. Soc.*, 2016, **138**, 14864–14867.
26 W. Ren, J. Huang, J. Ou, X. Sheng, Y. Shi, K. Huang and Y. Shi, *J. Org. Chem.*, 2025, **90**, 6334–6338.
27 W. Ren, Y. Liu, J. Ou, J. Huang, X. Sheng and Y. Shi, *J. Org. Chem.*, 2025, **90**, 8585–8595.
28 J. Li, G. Li, J. Li and Y. Shi, *Org. Lett.*, 2025, **27**, 6937–6941.
29 L. Liu, X.-C. Chen, S.-Q. Yang, Y.-Q. Yao, Y. Lu and Y. Liu, *J. Catal.*, 2021, **394**, 406–415.

30 A. Behr and L. Johnen, in *Handbook of Green Chemistry*, 2012, part 7, pp. 69–92.

31 E. V. Gusevskaya, J. Jiménez-Pinto and A. Börner, *ChemCatChem*, 2014, **6**, 382–411.

32 W. Schwab, C. Fuchs and F.-C. Huang, *Eur. J. Lipid Sci. Technol.*, 2013, **115**, 3–8.

33 F. G. Delolo, T. P. Moreira, A. d. O. Dias, E. N. dos Santos and E. V. Gusevskaya, *J. Catal.*, 2024, **432**, 115437.

34 C. Fan, J. Hou, Y. J. Chen, K. L. Ding and Q. L. Zhou, *Org. Lett.*, 2021, **23**, 2074–2077.

35 T. Sakakura, J.-C. Choi and H. Yasuda, *Chem. Rev.*, 2007, **107**, 2365–2387.

36 M. L. T. Triviño, N. C. Arriola, Y. S. Kang and J. G. Seo, *Chem. Eng. J.*, 2024, **487**, 150369.

37 K.-i. Tominaga and Y. Sasaki, *Catal. Commun.*, 2000, **1**, 1–3.

38 X. Ren, Z. Zheng, L. Zhang, Z. Wang, C. Xia and K. Ding, *Angew Chem. Int. Ed. Engl.*, 2017, **56**, 310–313.

39 A. G. Wu, J. Ding, L. Zhao, H. R. Li and L. N. He, *ChemSusChem*, 2024, **17**, e202400608.

40 R. Sang, Y. Hu, R. Razzaq, G. Mollaert, H. Atia, U. Bentrup, M. Sharif, H. Neumann, H. Junge, R. Jackstell, B. U. W. Maes and M. Beller, *Nat. Commun.*, 2022, **13**, 4432.

41 K. Hua, X. Liu, B. Wei, Z. Shao, Y. Deng, L. Zhong, H. Wang and Y. Sun, *Green Chem.*, 2021, **23**, 8040–8046.

42 Y. Li, S. Song and S. M. Sadeghzadeh, *Catal. Lett.*, 2022, **153**, 95–103.

43 G. Wang, M. Jiang, Z. Sun, L. Qian, G. Ji, L. Ma, C. Li, Z. Wang, Y. Yang, X. Lin, L. Yan and Y. Ding, *Chem. Eng. J.*, 2023, **476**, 146332.

44 G. Ji, C. Li, B. Fan, G. Wang, Z. Sun, M. Jiang, L. Ma, L. Yan and Y. Ding, *Chem. Eng. J.*, 2025, **522**, 168003.

45 J. Sun, K. Zhao, H. Wang and F. Shi, *ACS Sustain. Chem. Eng.*, 2024, **12**, 12736–12743.

46 J. Zhang, X. Kang, Y. Yan, X. Ding, L. He and Y. Li, *Angew Chem. Int. Ed. Engl.*, 2024, **63**, e202315777.

47 B. J. Jolly, M. J. Pung and C. Liu, *Dalton Trans.*, 2024, **53**, 18834–18838.

48 S. Yang, J. Zhao, X. Nie, X. Zheng, X. Xie, X. Zheng, H. Fu, H. Chen, R. Li, W. Xue and J. Xu, *Chem. Commun.*, 2025, **61**, 17165–17168.

49 Y. Tanabe, H. Sugisawa, T. Miyazawa, K. Hotta, K. Shiratori and T. Fujitani, *J. Chem. Inf. Model.*, 2025, **65**, 2245–2250.